PLOS ONE

RESEARCH ARTICLE

Computational study of parameter sensitivity in DevR regulated gene expression

Jagannath Das[1], Tarunendu Mapder[1¤], Sudip Chattopadhyay[1]*, Suman K. Banik[2]*

1 Department of Chemistry, Indian Institute of Engineering Science and Technology, Shibpur, Howrah, India, **2** Department of Chemistry, Bose Institute, Kolkata, India

¤ Current address: ARC centre of Excellence for Mathematical and Statistical Frontiers, School of Mathematical Sciences, Queensland University of Technology, Brisbane, QLD, Australia.
* sudip@chem.iiests.ac.in (SC); skbanik@jcbose.ac.in (SKB)

Citation: Das J, Mapder T, Chattopadhyay S, Banik SK (2020) Computational study of parameter sensitivity in DevR regulated gene expression. PLoS ONE 15(2): e0228967. https://doi.org/10.1371/journal.pone.0228967

Editor: Mingyang Lu, Jackson Laboratory, UNITED STATES

Received: July 26, 2019

Accepted: January 27, 2020

Published: February 13, 2020

Data Availability Statement: All relevant data are within the paper and its Supporting Information files.

Funding: Jagannath Das is thankful to Indian Institute of Engineering Science and Technology, Shibpur, Howrah, India, for a research fellowship. Suman K Banik acknowledges research support from Bose Institute, Kolkata, India. The funders had no role in study design, data collection and analysis, decision to publish, or preparation of the manuscript.

Abstract

The DevRS two-component system plays a pivotal role in signal transmission and downstream gene regulation in *Mycobacterium tuberculosis*. Under the hypoxic condition, phosphorylated DevR interacts with multiple binding sites at the promoter region of the target genes. In the present work, we carried out a detailed computational analysis to figure out the sensitivity of the kinetic parameters. The set of kinetic parameters takes care of the interaction among phosphorylated DevR and the binding sites, transcription and translation processes. We employ the method of stochastic optimization to quantitate the relevant kinetic parameter set necessary for DevR regulated gene expression. Measures of different correlation coefficients provide the relative ordering of kinetic parameters involved in gene regulation. Results obtained from correlation coefficients are further corroborated by sensitivity amplification.

Introduction

Tuberculosis is the second most infectious disease in today's world and is caused by the human pathogen *Mycobacterium tuberculosis* [1]. This highly studied pathogen kills around two million people each year. It is believed that approximately one-third of the world population carries *M. tuberculosis* bacteria within the human body in the inactive state, *viz*. dormant state. Different kinds of environmental and chemical factors trigger its activation. In the development of mycobacterial dormancy and latent tuberculosis, the two-component systems (TCS) plays a pivotal role. Here, it is relevant to note that the TCS is the most important signal transduction pathway in bacteria [2–4]. It is reported that in *M. tuberculosis* there are 11 well defined TCS [5]. The most studied among these TCSs is DevRS and is responsible for the dormancy of *M. tuberculosis* in the host. Analogous to the other TCS, DevRS contains a membrane-bound sensor kinase DevS and a cytoplasmic response regulator DevR. The sensor protein DevS utilizes adenosine triphosphate (ATP) to autophosphorylate a conserved histidine residue under hypoxic, nitric oxide, carbon monoxide, ascorbic acid environment or nutrient starvation conditions. The high energy phosphoryl group is then transferred to the conserved aspartate residue in DevR, the response regulator. Phosphorylated DevR (R_P)

Competing interests: The authors have declared that no competing interests exist.

regulates expression of ∼48 genes along with its operon. Several of these genes contain 20 bp palindromic sequence in the upstream region, known as Dev box, to which R_P binds [6].

In the present work, we undertake a computational approach to study interactions between R_P and four of its target genes, e.g., *Rv3134c*, *hspX*, *narK2* and *Rv1738*. A recent report by Chauhan et al [6] provides detailed information about the biochemical interactions between R_P and the four target genes. Based on the affinity of the binding strength of R_P to the binding sites present in the promoter region, the binding sites are broadly classified into two different classes, primary and secondary (see Fig 1). The main objectives of the present communication are two-fold. First, using simulated annealing, a stochastic optimization technique, we optimize the kinetic rate parameters. The optimized parameter set is then used to generate novel experimental profiles [7]. Second, we carried out a sensitivity analysis to figure out the sensitivity of the kinetic parameters related to the binding/unbinding constants, the rate of mRNA production from the promoter-GFP construct and rate of GFP production. Based on the correlation coefficient between the kinetic parameters and the output (GFP), we provide a detailed ordering of the parameters related to the expression of four target genes shown in Fig 1. The analysis based on correlation data sheds light on the complex interaction between DevR and the binding sites and shows how the binding sites are responsible for the gene expression. The sensitivity of the kinetic parameters is then further verified using the measure of sensitivity amplification.

Before proceeding further, we discuss here some of the theoretical developments related to the role of kinetic parameters in gene expression. Recently a computational method, sRACIPE, has been developed to implement stochastic analysis in random circuit perturbation method

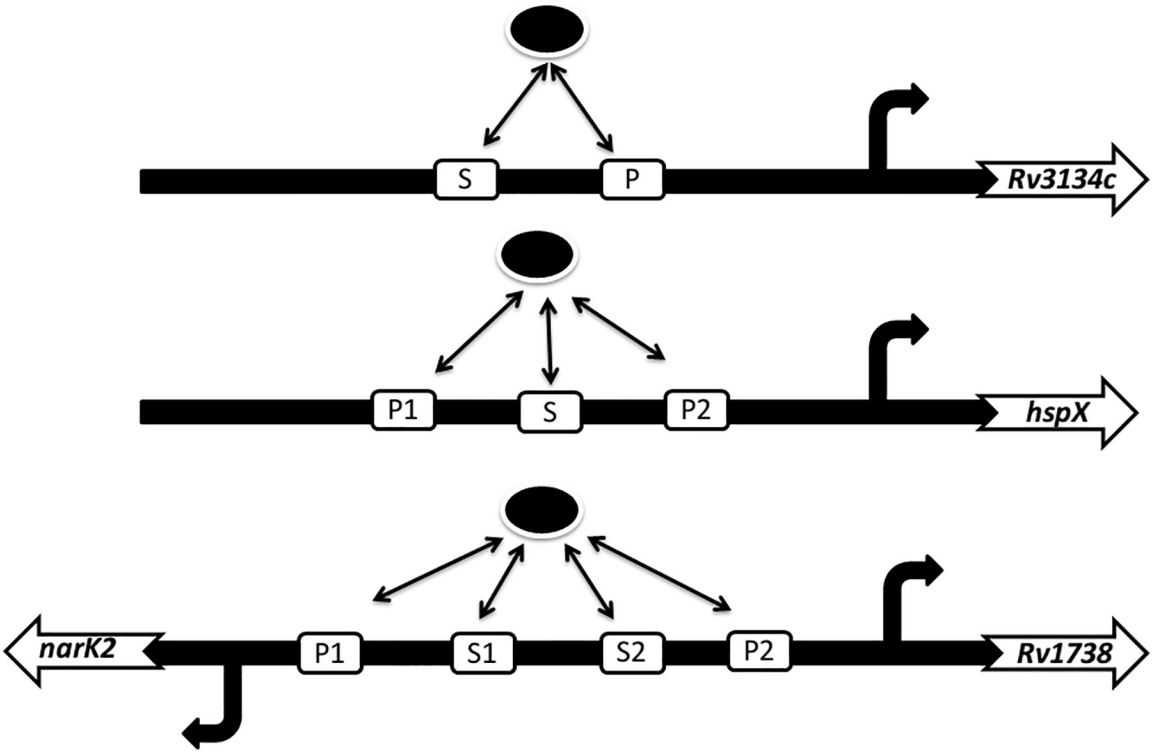

Fig 1. DevR-promoter interaction. Schematic diagram for interaction of phosphorylated DevR (black oval) with different binding sites of the target promoters. Promoters of *Rv3134c* and *hspx* contain two and three binding sites, respectively. A single promoter with four binding sites is shared by *narK2* and *Rv1738*. S (S1 and S2) and P (P1 and P2) stand for secondary and primary binding site, respectively [6].

https://doi.org/10.1371/journal.pone.0228967.g001

(RACIPE) [8]. sRACIPE takes care of noisy gene expression along with the parametric variation of a gene regulatory circuit while considering only its topology. The method developed is useful for studying multi-stable biological processes that exhibit fluctuations induced cell-to-cell variation in a cellular population. Implementation of global sensitivity analysis has been addressed earlier to engineer artificial genetic circuits [9] where the authors made an estimation of circuit properties in terms of model parameters, without prior knowledge of precise parameter values. Role of parameter robustness has also been investigated in neurogenic network [10]. A Monte Carlo based computation tool has been developed to identify regions of parameter space that can generate multi-stable states while taking into account fluctuations in parameter space and initial conditions [11].

Model and methods

Kinetic model

Based on the available experimental information [6] on interactions of DevR with the promoters of *Rv3134c*, *hspX*, *narK2* and *Rv1738* we employ the kinetic model [12]. The generalized kinetic scheme for phosphorylated DevR (R_P) regulated gene expression can be written as

$$\begin{aligned} P_i + R_p &\underset{k_{ui}}{\overset{k_{bi}}{\rightleftharpoons}} P_i^*, \\ P_i^* &\xrightarrow{k_{smi}} P_i^* + mGFP, \\ P_i^* \ldots P_N^* &\xrightarrow{k_{smc}} P_i^* \ldots P_N^* + mGFP, \\ mGFP &\xrightarrow{k_{d,m}} \phi, \\ mGFP &\xrightarrow{k_{sg}} mGFP + GFP \\ GFP &\xrightarrow{k_{dg}} \phi. \end{aligned}$$

The above kinetic scheme is valid for a promoter site with N numbers of binding sites ($i = 1 \ldots N$). P_i and P_i^* stands for the inactive and active state of the promoter, respectively. It is relevant to note that, in our model, each of the P_i-s represent the primary and/or secondary binding sites. *mGFP* and *GFP* are for mRNA and GFP, respectively. The kinetic scheme mentioned above needs to be translated into sets of coupled ordinary differential equations (ODEs) to investigate the steady state and temporal dynamics. For detailed kinetic rate equations with associated parameters, we refer to S1 Text and S1 Table.

Stochastic optimization: Simulated annealing

In this work, we adopted simulated annealing (SA) [13, 14], one of the prime stochastic optimization techniques to decipher the correct kinetic parameter set associated with the model. The algorithm of SA was developed using the notion adopted in metallurgy. In the metallurgical annealing process, a molten mixture of metals by quickly lowering the temperature leads to a defective crystal structure of the target alloy, far from the minimum Gibbs free energy state. Starting from a high temperature, cooling must be slow when approaching the recrystallization temperature to obtain a nearly-perfect defect-free crystal, which is a crystal close to the minimum energy state.

In analogy with the metallurgical annealing, here we make use of an algorithmic temperature called annealing temperature T_{at}. The extent of search space which is being sampled is determined by the magnitude of annealing temperature. Considering Boltzmann distribution

to simulate the behavior of the ensemble, the probability of the energy state of the system at temperature T is given by $p(E_0) = \exp(-E_0/k_BT)/Z(T)$, where E_0 is the energy of the state, k_B is Boltzmann constant and $Z(T)$ is the normalization factor. We define a cost function or objective function Δ to follow the progress of the search towards the solution. While carrying out the optimization, in each iteration, a small random move is applied to a random kinetic parameter, and the subsequent difference in Δ is estimated. If $\Delta \leq 0$ the new state is always accepted. On the other hand, if $\Delta > 0$ the state can be accepted with some probability to escape from the local minima, using the principle of Metropolis test [15]. The transition probability of accepting the later type of solution ($\Delta > 0$) is $F(T_{at}) = \exp(-\Delta/T_{at})$. In every iteration $F(T_{at})$ is compared with a random number between 0 and 1. If the value of $F(T_{at})$ is greater than the random number, the solution is accepted, otherwise rejected. The physical reasoning behind this criterion is that if $F(T_{at})$ is greater than the invoked random number between 0 and 1, the move is more probable than a random event which in the present case is the generation of a random number. If a solution is rejected, then another neighbouring solution is generated and evaluated. The persistence of each temperature level regulates the number of iterations at a particular temperature. The temperature reduction takes place during the search process according to a cooling schedule, and the process terminates after reaching a specified (target) lowest temperature.

Sensitivity analysis: Correlation coeffcient

Presence of variability in the experimental data often brings in the complication in the proper estimation of kinetic parameters associated with model biological systems. To identify and subsequent quantification of the relevant model parameters we adopt the method of sensitivity analysis [16–20]. In the present report, we quantify the sensitivity of each parameter of the model using the measure of a different correlation coefficient.

Here, we calculate three types of correlation coefficients, namely Pearson correlation coefficient (CC), Spearman rank correlation coefficient (RCC) and, partial rank correlation coefficient (PRCC). Usage of CC is appropriate in case of linear dependence, but in the case of nonlinear monotonic dependence, RCC gives more accurate results. In RCC, the correlation coefficient is calculated after a rank transformation of the data set. Correlation of a particular input parameter (from a set of parameters) with the output while excluding the effect of rest of the parameters is known as PRCC. PRCC between a particular input and the output thus excludes any effect of other model inputs. In other words, it is cleaned of any correlation between multiple inputs [16, 18]. Calculation of PRCC also takes care of sensitivity measure for the nonlinear but monotonic relationship between rank transformed data, hence making it the most efficient and reliable metric. It is important to mention that the strength of dependency between the input and the output is measured by the magnitude of the correlation coefficient, and it varies from -1 to +1. A low value signifies weak dependency, whereas a high value represents strong dependence. The negative values indicate anti-correlation between the input and the output. In the present report, the absolute magnitude of the correlation coefficient is a measure for the evaluation of the sensitivity of the input with respect to the output.

To quantify the correlation coefficients, all the optimized parameters reported in Table 1 have been perturbed randomly in order to solve the kinetic equations (see Eqs. (S41-S58) in S1 Text). The random perturbation is drawn from a Gaussian distribution. The mean and the variance of the Gaussian distribution is the base value of the parameter and is ±5% (and ±10%, see S2–S6 Tables) of the base value, respectively. The kinetic equations with a perturbed set of parameters are solved numerically using numerical ODE solver `NDSolve` of Mathematica

Table 1. List of optimized parameters associated with DevR regulated gene expression. Here, $x \pm y$ stands for the value of optimized parameter x with standard deviation y. The standard deviation is evaluated using the data of 10^3 independent SA simulations. Parameter values tabulated in Set 1 and Set 2 are due to different sets of random initial conditions. Parameters shown under Mean is the average values of Set 1 and Set 2.

Parameter	Set 1	Set 2	Mean	Unit
k_{srp}	$(2.89 \pm 0.54) \times 10^{-3}$	$(3.41 \pm 0.68) \times 10^{-3}$	$(3.15 \pm 0.61) \times 10^{-3}$	nM s^{-1}
k_{drp}	$(5.16 \pm 1.13) \times 10^{-5}$	$(4.75 \pm 0.88) \times 10^{-5}$	$(4.96 \pm 1.01) \times 10^{-5}$	s^{-1}
k_{b1}	$(3.81 \pm 0.54) \times 10^{-7}$	$(3.13 \pm 0.69) \times 10^{-7}$	$(3.47 \pm 0.62) \times 10^{-7}$	$nM^{-1}s^{-1}$
k_{u1}	$(4.12 \pm 0.91) \times 10^{-8}$	$(4.72 \pm 0.88) \times 10^{-8}$	$(4.42 \pm 0.90) \times 10^{-8}$	s^{-1}
k_{b2}	$(3.48 \pm 0.45) \times 10^{-7}$	$(3.40 \pm 0.75) \times 10^{-7}$	$(3.44 \pm 0.60) \times 10^{-7}$	$nM^{-1}s^{-1}$
k_{u2}	$(4.50 \pm 0.99) \times 10^{-8}$	$(5.59 \pm 1.05) \times 10^{-8}$	$(5.05 \pm 1.02) \times 10^{-8}$	s^{-1}
k_{b3}	$(3.43 \pm 0.66) \times 10^{-7}$	$(2.81 \pm 0.55) \times 10^{-7}$	$(3.12 \pm 0.61) \times 10^{-7}$	$nM^{-1}s^{-1}$
k_{u3}	$(5.58 \pm 1.17) \times 10^{-7}$	$(4.44 \pm 0.67) \times 10^{-7}$	$(5.01 \pm 0.92) \times 10^{-7}$	s^{-1}
k_{b4}	$(4.76 \pm 0.84) \times 10^{-7}$	$(3.72 \pm 0.67) \times 10^{-7}$	$(4.24 \pm 0.76) \times 10^{-7}$	$nM^{-1}s^{-1}$
k_{u4}	$(4.49 \pm 0.72) \times 10^{-7}$	$(5.84 \pm 0.89) \times 10^{-7}$	$(5.17 \pm 0.81) \times 10^{-7}$	s^{-1}
k_{b5}	$(3.80 \pm 0.80) \times 10^{-7}$	$(3.00 \pm 0.56) \times 10^{-7}$	$(3.40 \pm 0.68) \times 10^{-7}$	$nM^{-1}s^{-1}$
k_{u5}	$(4.28 \pm 0.76) \times 10^{-7}$	$(4.13 \pm 0.71) \times 10^{-7}$	$(4.21 \pm 0.74) \times 10^{-7}$	s^{-1}
k_{b6}	$(4.25 \pm 0.72) \times 10^{-7}$	$(4.77 \pm 0.80) \times 10^{-7}$	$(4.51 \pm 0.76) \times 10^{-7}$	$nM^{-1}s^{-1}$
k_{u6}	$(4.59 \pm 0.78) \times 10^{-7}$	$(5.85 \pm 0.89) \times 10^{-7}$	$(5.22 \pm 0.84) \times 10^{-7}$	s^{-1}
k_{b7}	$(3.52 \pm 0.73) \times 10^{-7}$	$(2.85 \pm 0.49) \times 10^{-7}$	$(3.19 \pm 0.61) \times 10^{-7}$	$nM^{-1}s^{-1}$
k_{u7}	$(5.30 \pm 0.90) \times 10^{-7}$	$(6.33 \pm 0.97) \times 10^{-7}$	$(5.82 \pm 0.94) \times 10^{-7}$	s^{-1}
k_{b8}	$(4.12 \pm 0.71) \times 10^{-7}$	$(3.66 \pm 0.55) \times 10^{-7}$	$(3.89 \pm 0.63) \times 10^{-7}$	$nM^{-1}s^{-1}$
k_{u8}	$(5.66 \pm 1.05) \times 10^{-7}$	$(3.98 \pm 0.58) \times 10^{-7}$	$(4.82 \pm 0.82) \times 10^{-7}$	s^{-1}
k_{b9}	$(3.53 \pm 0.64) \times 10^{-7}$	$(6.45 \pm 1.11) \times 10^{-7}$	$(4.99 \pm 0.88) \times 10^{-7}$	$nM^{-1}s^{-1}$
k_{u9}	$(4.19 \pm 0.74) \times 10^{-7}$	$(4.47 \pm 0.69) \times 10^{-7}$	$(4.33 \pm 0.72) \times 10^{-7}$	s^{-1}
k_{sm1}	$(0.60 \pm 0.21) \times 10^{-3}$	$(1.20 \pm 0.13) \times 10^{-3}$	$(0.9 \pm 0.17) \times 10^{-3}$	nM s^{-1}
k_{sm2}	$(7.12 \pm 1.54) \times 10^{-4}$	$(4.10 \pm 0.86) \times 10^{-4}$	$(5.61 \pm 1.20) \times 10^{-4}$	nM s^{-1}
k_{sm3}	$(6.19 \pm 0.28) \times 10^{-3}$	$(5.57 \pm 1.56) \times 10^{-3}$	$(5.88 \pm 0.92) \times 10^{-3}$	nM s^{-1}
k_{sm4}	$(4.39 \pm 0.85) \times 10^{-3}$	$(4.83 \pm 0.71) \times 10^{-3}$	$(4.61 \pm 0.78) \times 10^{-3}$	nM s^{-1}
k_{sm5}	$(0.46 \pm 0.09) \times 10^{-3}$	$(1.21 \pm 0.36) \times 10^{-3}$	$(0.84 \pm 0.23) \times 10^{-3}$	nM s^{-1}
k_{sm6}	$(1.14 \pm 0.39) \times 10^{-3}$	$(0.92 \pm 0.34) \times 10^{-3}$	$(1.03 \pm 0.37) \times 10^{-3}$	nM s^{-1}
k_{sm7}	$(7.14 \pm 1.00) \times 10^{-3}$	$(5.13 \pm 0.68) \times 10^{-3}$	$(6.14 \pm 0.84) \times 10^{-3}$	nM s^{-1}
k_{sm8}	$(6.13 \pm 1.08) \times 10^{-4}$	$(3.97 \pm 0.60) \times 10^{-4}$	$(5.05 \pm 0.84) \times 10^{-4}$	nM s^{-1}
k_{sm9}	$(4.44 \pm 0.73) \times 10^{-4}$	$(4.42 \pm 0.71) \times 10^{-4}$	$(4.43 \pm 0.72) \times 10^{-4}$	nM s^{-1}
k_{sm10}	$(4.82 \pm 0.96) \times 10^{-5}$	$(3.88 \pm 0.53) \times 10^{-5}$	$(4.35 \pm 0.75) \times 10^{-5}$	nM s^{-1}
k_{sm11}	$(3.79 \pm 0.76) \times 10^{-3}$	$(3.13 \pm 0.54) \times 10^{-3}$	$(3.46 \pm 0.65) \times 10^{-3}$	nM s^{-1}
k_{sm12}	$(6.00 \pm 1.08) \times 10^{-5}$	$(5.87 \pm 0.93) \times 10^{-5}$	$(5.94 \pm 1.01) \times 10^{-5}$	nM s^{-1}
k_{sm13}	$(4.82 \pm 0.86) \times 10^{-5}$	$(6.06 \pm 0.90) \times 10^{-5}$	$(5.44 \pm 0.88) \times 10^{-5}$	nM s^{-1}
k_{sm14}	$(5.97 \pm 1.17) \times 10^{-5}$	$(6.00 \pm 0.90) \times 10^{-5}$	$(5.99 \pm 1.04) \times 10^{-5}$	nM s^{-1}
k_{sm15}	$(4.95 \pm 0.83) \times 10^{-4}$	$(4.72 \pm 0.73) \times 10^{-4}$	$(4.84 \pm 0.78) \times 10^{-4}$	nM s^{-1}
k_{sm16}	$(5.79 \pm 1.05) \times 10^{-4}$	$(4.12 \pm 0.73) \times 10^{-4}$	$(4.96 \pm 0.89) \times 10^{-4}$	nM s^{-1}
k_{sm17}	$(6.26 \pm 1.17) \times 10^{-3}$	$(5.94 \pm 0.96) \times 10^{-3}$	$(6.10 \pm 0.97) \times 10^{-3}$	nM s^{-1}
k_{sm18}	$(5.24 \pm 0.91) \times 10^{-4}$	$(7.26 \pm 1.11) \times 10^{-4}$	$(6.25 \pm 1.01) \times 10^{-4}$	nM s^{-1}
k_{sm19}	$(4.38 \pm 0.83) \times 10^{-3}$	$(4.93 \pm 0.83) \times 10^{-3}$	$(4.66 \pm 0.83) \times 10^{-3}$	nM s^{-1}
k_{dm}	$(4.34 \pm 0.86) \times 10^{-4}$	$(3.74 \pm 0.60) \times 10^{-4}$	$(4.04 \pm 0.73) \times 10^{-4}$	s^{-1}
k_{sg}	$(5.03 \pm 0.92) \times 10^{-4}$	$(3.79 \pm 0.55) \times 10^{-4}$	$(4.41 \pm 0.74) \times 10^{-4}$	nM s^{-1}
k_{dg}	$(2.75 \pm 0.57) \times 10^{-5}$	$(2.62 \pm 0.51) \times 10^{-5}$	$(2.69 \pm 0.54) \times 10^{-5}$	s^{-1}

https://doi.org/10.1371/journal.pone.0228967.t001

(version 11.3, Wolfram Inc.) till the system reaches steady state. After each simulation, the steady state value of GFP is collected to figure out its dependency on a particular parameter value. To calculate the correlation coefficients between the parameter-GFP pair, we carried out 10^6 independent simulation.

Sensitivity amplification

To further check the role of kinetic parameters in gene expression, we employ the measure of sensitivity amplification [21–23]. Sensitivity amplification is the relative percentage change in response with respect to the percentage change in stimulus. In the present study, a change in the GFP level is considered as a response while a change in the kinetic rate parameters is considered as a variation of the stimulus. Considering this we define sensitivity amplification

$$A_S = \frac{\Delta GFP/GFP^i}{\Delta k/k^i},$$

with $\Delta GFP = GFP^f - GFP^i$ and $\Delta k = k^f - k^i$ where i and f stand for the initial and final value, respectively.

Results and discussions

Optimization of the kinetic parameters

One of the main goals of the current work is to obtain the right set of kinetic parameters relevant to DevR controlled gene expression. In this context, it is essential to mention that parameters related to the current project are unavailable in the literature. To the best of our knowledge, only experimental information we have at our disposal is gene expression of wild type and some mutants [7, 24]. Keeping this in mind, we carried out stochastic optimization of the full kinetic parameter set. During simulation optimization of each parameter k (say) is done using the relation

$$k' = k + k \times (-1)^n \times \delta \times r_n,$$

with k' being the updated value of k. Here, n is a random integer, δ is the amplitude of allowed change of a selected parameter which in our case lies between 0.01 to 0.05, and r_n is a random integer between 0 and 1. As mentioned in Sec 2.2 we calculated a cost function or objective function for the new set of updated variables in each iteration. For *Rv3134c* and *hspX* we use the cost function

$$\Delta = \sum_{i=1}^{N} (G_i^{\exp} - G_i^{T_{at}})^2.$$

Here $G_i^{\exp}$ is the experimental (target) GFP value and $G_i^{T_{at}}$ is the simulated GFP value at the annealing temperature T_{at} evaluated at the i-th step of the simulation. Due to common sharing of the promoter we use the following cost function for *narK2-Rv1738* system

$$\Delta = \alpha \sum_{i=1}^{N} (G_i^{\exp} - G_i^{T_{at}})^2 + \beta \sum_{i=1}^{N} (G_i^{\exp} - G_i^{T_{at}})^2,$$

where α and β are scalar weights. In the present problem, we set $\alpha = \beta = 1$.

Following the above structures of the cost function, we carried out the simulation. Initially, we ascribed random initial values to the model parameters to execute the simulation. To check whether different sets of initial conditions lead to a unique parameter set, we performed simulation using two different random sets of initial conditions (please see the end of S1 Text). The two resultant optimized parameter sets are given in Table 1. In addition, Table 1 also shows the mean of the two parameter sets. The optimized parameters were then used to generate the experimental GFP expression profiles of all the target genes (see Fig 2) reported by Chauhan and Tyagi [7]. The corresponding steady state levels of GFP are shown in Fig 3A. We note that

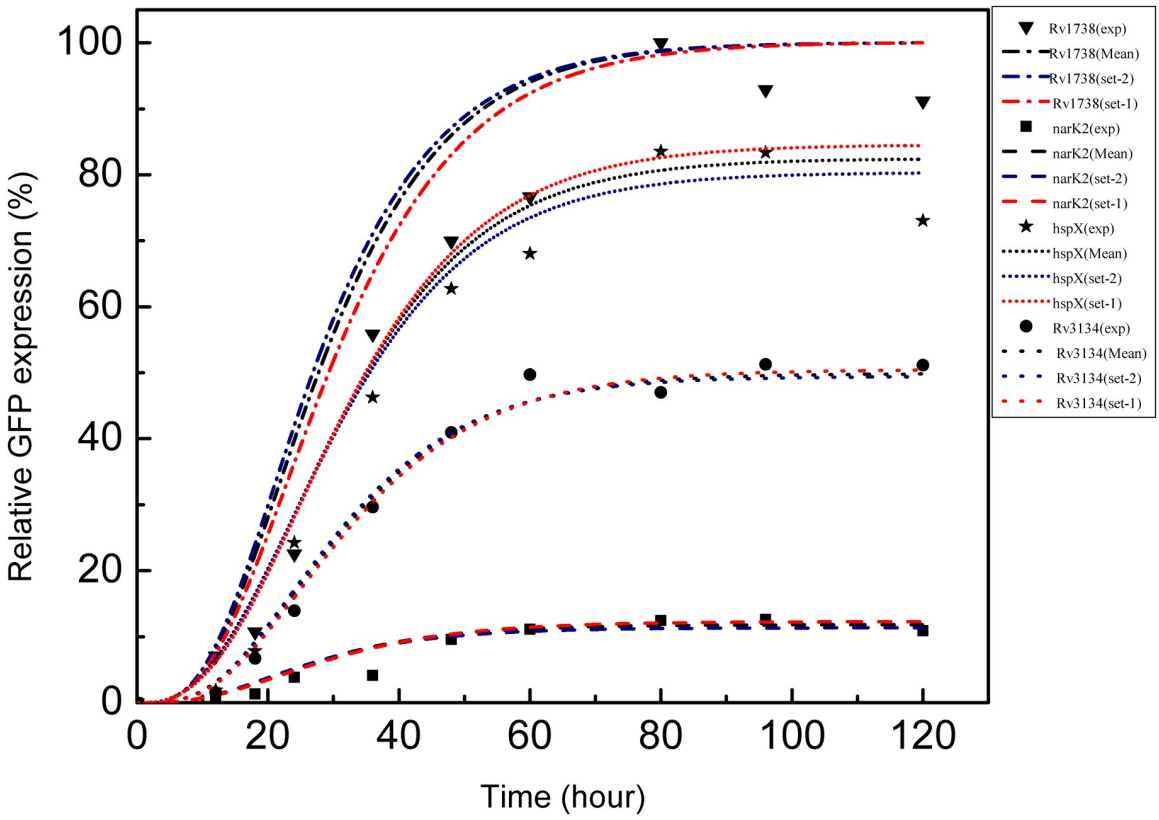

Fig 2. Temporal gene expression. Temporal GFP expression of *Rv3134c*, *hspx*, *narK2* and *Rv1738*. The symbols are taken from Chauhan and Tyagi [7] and the lines are generated using optimized set of parameters shown in Table 1. Red and blue lines are drawn using Set 1 and Set 2, respectively. The black lines are due to Mean values reported in Table 1.

https://doi.org/10.1371/journal.pone.0228967.g002

the parameter values reported in these two sets although look different, they, however, generate similar kind of temporal profiles as shown in Fig 2. The profiles of cost function and evolution of kinetic rate parameters are shown in Fig 4 and S1–S3 Figs, respectively. We note that the experimental values plotted in Fig 2 show reduced expression at later time points ($\sim$ 90 −120 hrs). Multiple reasons may cause such reduction, e.g., cell death due to limited resources, dilution effect, etc. [25].

To generate the desired optimized set of parameters, we carried out 10^3 independent SA runs. In each independent simulation, the initial annealing temperature T_{at} was set at 300 along with 1% rate of cooling (annealing schedule). The number of SA steps in each simulation was 10^4. Multiple SA runs are essential because the upgradation of parameter values in the model is done by using random numbers and in a given run, there is a finite possibility that the updated parameters are not able to cause a reduction in the cost function value by a substantial amount. However, if a large number of SA runs are executed as has been done in the present study, precise upgradation will happen in certain trajectories with the associated decrease in cost function quickly and towards the desired solution.

Sensitivity of the kinetic parameters

After optimization of the full kinetic parameter set, we focus on finding out the sensitivity of the same in connection to gene expression. To this end, we first quantify the correlation between the GFP level of the four target genes with the synthesis (k_{srp}) and degradation (k_{drp})

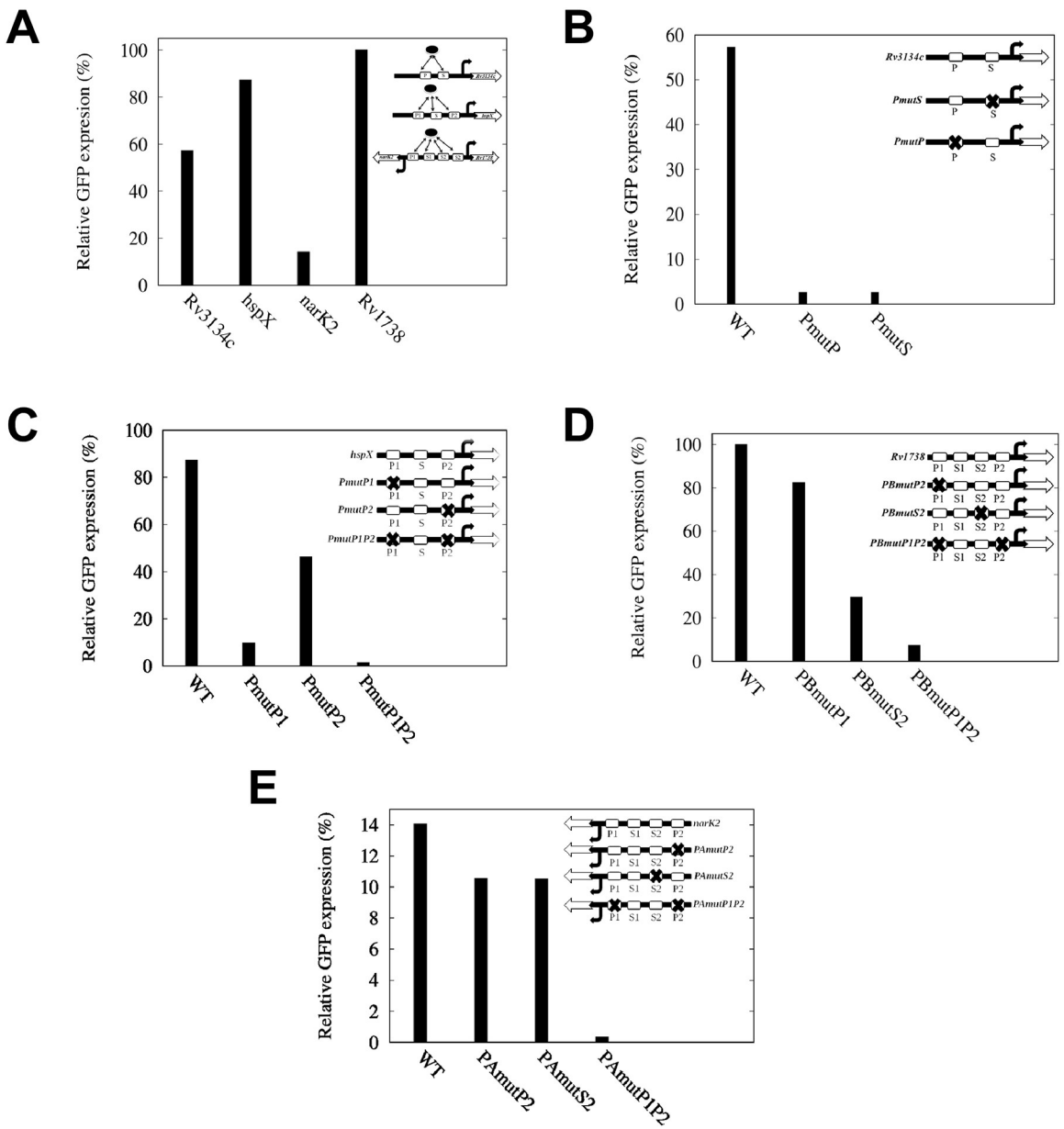

Fig 3. Relative gene expression at steady state. A.*Rv3134c*, *hspX*, *narK2* and *Rv1738*. **B**. *Rv3134c* and mutants. **C**. *hspX* and mutants. **D**. *Rv1738* and mutants, and **E**. *narK2* and mutants.

https://doi.org/10.1371/journal.pone.0228967.g003

rate of the transcription factor R_P. We also calculate the correlation of the GFP level with the synthesis (k_{sg}) and degradation (k_{dg}) rate of the GFP itself. As discussed in Sec 2.3, all the parameters have been perturbed randomly to solve the kinetic equations (using the perturbed set of parameters). A Representative of 10^3 simulation data are shown as scatter plots in S4 Fig. The nature of scatter plots suggests that the synthesis and the degradation rate of the transcription factor have a weak effect on the GFP level. However, the synthesis and degradation rate of GFP shows a prominent positive and negative correlation, respectively. To quantify the correlation, we calculate CC, RCC and PRCC for all the four genes and are tabulated in Table 2. Here the correlation values have been calculated using 10^6 independent trajectories. While

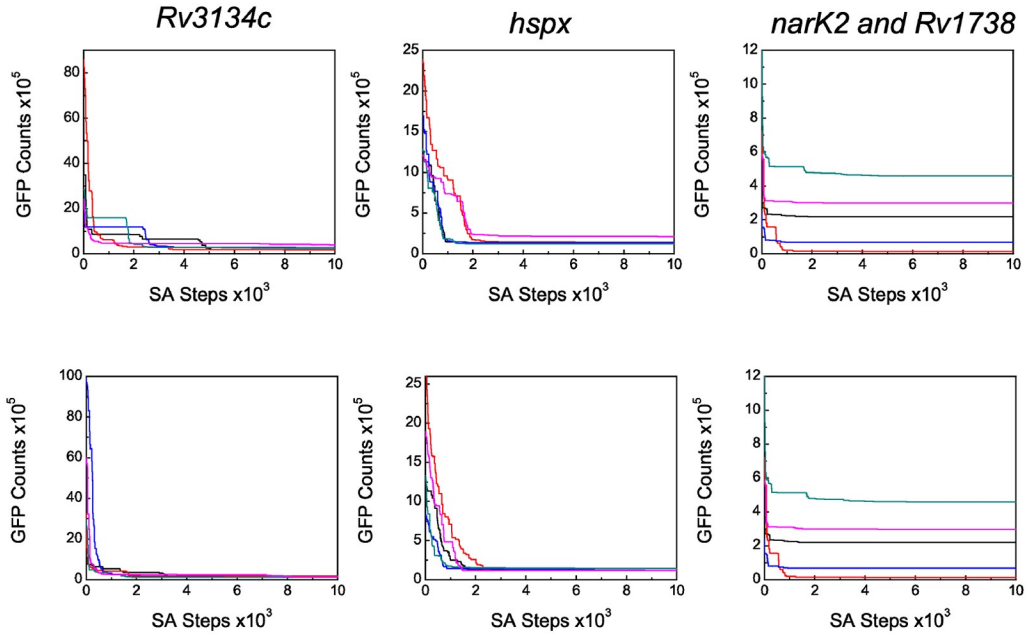

Fig 4. Evolution of cost function. The cost function of GFP counts as a function of SA steps associated with *Rv3134c*, *hspx*, *narK2* and *Rv1738*. The five solid lines are generated from five different SA runs and are representatives of 10^3 simulation. Top and bottom panels are due to Set 1 and Set 2 parameters, respectively.

https://doi.org/10.1371/journal.pone.0228967.g004

quantifying the correlation values, we have used both the parameter sets (i.e., Set 1 and Set 2) shown in Table 1. As a result, each measure of correlation coefficients has three entries in Table 2. We adopted the same strategy for measuring correlation values for other model parameters. The correlation values listed in Table 2 suggests an ordering of the target genes output (GFP level) for each of the four parameters (k_{srp}, k_{drp}, k_{sg} and k_{dg})

$$\begin{aligned} k_{srp} &: Rv3134c < narK2 \sim Rv1738 \sim hspX, \\ k_{drp} &: Rv3134c < narK2 \sim Rv1738 \sim hspX, \\ k_{sg} &: Rv3134c \sim narK2 \sim Rv1738 \sim hspX, \\ k_{dg} &: Rv3134c \sim narK2 \sim Rv1738 \sim hspX. \end{aligned}$$

Table 2. CC, RCC, PRCC values for synthesis and degradation rate of four genes using 5% perturbation.

		Rv3134c			*hspX*			*narK2*			*Rv1738*		
	Parameter	**CC**	**RCC**	**PRCC**	**CC**	**RCC**	**PRCC**	**CC**	**RCC**	**PRCC**	**CC**	**RCC**	**PRCC**
Set 1	k_{srp}	0.010	0.010	0.028	0.029	0.028	0.098	0.025	0.023	0.083	0.027	0.026	0.100
	k_{drp}	-0.006	-0.004	-0.023	-0.020	-0.021	-0.100	-0.026	-0.025	-0.082	-0.026	-0.025	-0.088
	k_{sg}	0.516	0.500	0.886	0.536	0.523	0.895	0.549	0.534	0.900	0.546	0.531	0.898
	k_{dg}	-0.520	-0.504	-0.885	-0.539	-0.521	-0.895	-0.551	-0.534	-0.900	-0.547	-0.530	-0.898
Set 2	k_{srp}	-0.001	-0.001	0.014	0.022	0.021	0.084	0.016	0.016	0.068	0.019	0.019	0.074
	k_{drp}	0.002	0.003	-0.018	-0.021	-0.020	-0.077	-0.018	-0.017	-0.068	-0.017	-0.017	-0.078
	k_{sg}	0.523	0.508	0.888	0.543	0.529	0.897	0.551	0.536	0.900	0.547	0.532	0.899
	k_{dg}	-0.525	-0.507	-0.888	-0.546	-0.527	-0.896	-0.549	-0.531	-0.899	-0.545	-0.527	-0.897
Mean	k_{srp}	0.005	0.005	0.021	0.026	0.025	0.091	0.021	0.020	0.076	0.023	0.023	0.087
	k_{drp}	-0.002	-0.001	-0.021	-0.021	-0.021	-0.089	-0.022	-0.021	-0.075	-0.022	-0.021	-0.083
	k_{sg}	0.520	0.504	0.887	0.540	0.526	0.896	0.550	0.535	0.900	0.574	0.532	0.899
	k_{dg}	-0.523	-0.506	-0.887	-0.543	-0.524	-0.896	-0.550	-0.533	-0.900	-0.546	-0.529	-0.898

https://doi.org/10.1371/journal.pone.0228967.t002

Table 3. CC, RCC, PRCC values for all the parameter of *Rv3134c*. The input parameters are calculated with output GFP using 5% perturbation.

	CC			RCC			PRCC		
Parameter	Set1	Set2	Mean	Set1	Set2	Mean	Set1	Set2	Mean
k_{dm}	-0.521	-0.523	-0.522	-0.505	-0.506	-0.506	-0.887	-0.887	-0.887
k_{sm3}	0.428	0.403	0.416	0.413	0.391	0.402	0.844	0.830	0.837
k_{sm1}	0.044	0.090	0.067	0.043	0.087	0.065	0.150	0.304	0.227
k_{sm2}	0.050	0.028	0.039	0.049	0.030	0.040	0.180	0.115	0.148
k_{b1}	0.008	0.009	0.008	0.007	0.009	0.008	0.023	0.024	0.023
k_{b2}	0.009	0.008	0.008	0.008	0.010	0.009	0.024	0.025	0.024
k_{u1}	0.003	-0.007	-0.002	0.001	-0.008	-0.004	-0.000	-0.013	-0.007
k_{u2}	-0.000	0.006	0.006	-0.006	-0.005	-0.005	-0.001	-0.003	-0.002

https://doi.org/10.1371/journal.pone.0228967.t003

Here we note that the synthesis rate k_{sg} is the translation rate of GFP from its mRNA. In the present model, k_{sg} is the same for all the target genes, which gets reflected in the almost equal correlation between k_{sg} and GFP. On a similar note correlation between k_{dg} and GFP becomes equal. The PRCC values reported in Table 2 are higher than CC and RCC values as calculation of PRCC excludes the effect of other parameters in the calculation.

Having figured out the sensitivity of the parameters associated with the transcription factor R_P, we focus on the parameters associated with the four target genes. The degradation rate of GFP (k_{dg}) shows the maximum level of correlation (negative) with GFP itself compared to the other parameters. We thus exclude k_{dg} while looking at the sensitivity of other parameters related to gene expression.

Two binding sites act co-oepratively in *RV3134c* expression. First, we analyse the sensitivity of the parameters related to *Rv3134c*. Using the previous strategy, we quantified the correlation between the parameters and the GFP level (Table 3). Here, the relative ordering of the parameters in terms of correlation values (absolute) are

$$k_{sm3} \gg k_{sm1} \sim k_{sm2} > k_{b1} \sim k_{b2} \gg k_{u1} \sim k_{u2}.$$

The above ordering suggests that both the primary (P) and secondary (S) binding sites are necessary for full activation of the *Rv3134c* gene. Such necessity gets reflected in the high correlation value associated with the parameter k_{sm3} taking care of co-operativity driven mRNA production. This is in agreement with the maximum level of GFP expression in the wild type strain reported by Chauhan and Tyagi [26]. Furthermore, the ordering $k_{sm3} \gg k_{sm1} \sim k_{sm2}$ suggests that mutation of one of the binding sites (P or S) reduces the correlation of k_{sm1} and k_{sm2} with the output (GFP). During the experiment when either of the binding sites is mutated, the mutants pmutP and pmutS show $\sim$25 fold less GFP expression compared to the wild type strain (Fig 3B) [26]. Correlation associated with the binding parameters k_{b1} and k_{b2} comes next and have minimal effect on the GFP level. The unbinding parameters k_{u1} and k_{u2} have the least contribution with an order of magnitude lower value of (negative) correlation.

Binding of R_P to distal site P1 acts as a bottleneck for *hspX* expression. Next, we check sensitivity of the parameters associated with *hspX*. The ordering of the parameters related to expression of *hspX* in terms of correlation values (absolute) (see Table 4) are

$$k_{sm4} > k_{sm7} > k_{sm5} > k_{sm6} \gg k_{b3} \sim k_{u3} > k_{b5} \sim k_{u4} \sim k_{u5} \sim k_{b4}.$$

In *hspX*, the synthesis rate k_{sm4} from the activated distal primary binding site P1 shows a maximum correlation with the output (GFP) compared to the other synthesis rates associated with *hspX*. On the other hand, the activation and inactivation rates (k_{b3} and k_{u3}) related to the

Table 4. CC, RCC, PRCC values for all the parameter of *hspX*. The input parameters are calculated with output GFP using 5% perturbation.

	CC			RCC			PRCC		
Parameter	Set1	Set2	Mean	Set1	Set2	Mean	Set1	Set2	Mean
k_{dm}	-0.538	-0.547	-0.543	-0.520	-0.530	-0.525	-0.895	-0.897	-0.896
k_{sm4}	0.286	0.227	0.257	0.276	0.219	0.248	0.729	0.639	0.684
k_{sm7}	0.182	0.218	0.200	0.175	0.211	0.193	0.562	0.630	0.596
k_{sm5}	0.048	0.043	0.046	0.046	0.041	0.044	0.177	0.154	0.166
k_{sm6}	0.014	0.057	0.036	0.015	0.055	0.035	0.078	0.205	0.142
k_{b3}	0.015	0.012	0.014	0.013	0.013	0.013	0.053	0.049	0.051
k_{u3}	-0.014	-0.007	-0.011	-0.013	-0.007	-0.010	-0.052	-0.030	-0.041
k_{b5}	0.010	0.011	0.011	0.011	0.010	0.011	0.032	0.014	0.023
k_{u4}	-0.001	-0.005	-0.003	-0.000	-0.004	-0.002	-0.022	-0.021	-0.022
k_{u5}	-0.002	-0.009	-0.006	-0.003	-0.009	-0.006	-0.023	-0.021	-0.022
k_{b4}	0.007	0.002	0.005	0.004	0.003	0.004	0.019	0.020	0.020

https://doi.org/10.1371/journal.pone.0228967.t004

formation of active P1 (P1*) show a lesser correlation. These two opposing factors work together to determine the effective contribution of distal binding site P1 in the expression of *hspX* as reported by Chauhan et al. [6]. In other words, K_D (= k_u/k_b) value associated with the distal binding site P1 acts as a bottleneck for its proper functionality. Due to this reason, the mutant pmutP1 (mutation at P1) showed $\sim$ 30% of the wild type GFP expression, as reported by Park et al. [24] (Fig 3C).

The next parameter that shows high correlation with GFP is k_{sm7} which takes care of synthesis of GFP due to the cooperative effect of all the three binding sites (P1, S and P2) of *hspX*. The synthesis rates k_{sm5} and k_{sm6} due to P2 and S, respectively, come next. As P2 lies close to the transcription start point (TSP) of *hspX*, the GFP synthesis rate due to P2 is higher than that of S. It is important to note that, mutation at P2 (pmutP2) shows $\sim$ 53% of the wild type expression. Thus mutation at both primary binding sites P1 and P2 (pmutP1P2) shows only $\sim$ 12% of wild type expression and agrees with Park et al. [24]. The correlation values due to binding (k_{b4} & k_{b5}) and unbinding (k_{u4} & k_{u5}) rates with GFP for the activation of P2 and S show that preference of R_P is almost equal for P2 and S due to their close proximity.

Promoter sharing reverses the role of binding sites in *narK2-Rv1738* system. Finally, we analyse the sensitivity of the parameters related to *narK2-Rv1738* system. For these pair of genes we quantify the correlation coefficients (Tables 5 and 6). The ordering of the parameters related to *narK2* in terms of absolute correlation values are (see Table 5)

$$k_{sm8} > k_{sm16} > k_{sm18} \gg k_{sm14} \sim k_{sm12} > k_{sm10} > k_{b6} \sim k_{b7} \sim k_{u6} \sim k_{u7} > k_{b9} \sim k_{u8} \sim k_{b8} \sim k_{u9}.$$

In *narK2*, the parameter with the highest correlation coefficient is k_{sm8}, related to transcription from the primary site P1. Thus deletion of P1 results in almost zero expression in the mutant pAmutP1 [7]. The next sensitive parameter is k_{sm16} that takes care of transcription from both P1 and S1. The parameter k_{sm18} is related to the transcription from the secondary binding sites P2 and S2. The low value of k_{sm18} compared to k_{sm8} and k_{sm16} is due to the distal nature of P2 and S2 from the TSP of *narK2*. The correlation ordering of k_{sm8} together with k_{sm16} and k_{sm18} shows that contribution of P2 and S2 in the expression of *narK2* is minimal and both are unable to rescue the low expression profile of pAmutP1. Due to the distal nature of P2 and S2 single mutation results in almost similar kind of expression in pAmutP2 and pAmutS2, respectively [7] (see Fig 3E).

Table 5. CC, RCC, PRCC values for all the parameter of *narK2*. The input parameters are calculated with output GFP using 5% perturbation.

	CC			RCC			PRCC		
Parameter	Set1	Set2	Mean	Set1	Set2	Mean	Set1	Set2	Mean
k_{dm}	-0.552	-0.546	-0.549	-0.535	-0.530	-0.533	-0.900	-0.900	-0.900
k_{sm8}	0.154	0.235	0.195	0.147	0.226	0.187	0.487	0.655	0.571
k_{sm16}	0.182	0.128	0.155	0.175	0.123	0.149	0.558	0.436	0.497
k_{sm18}	0.171	0.135	0.153	0.165	0.130	0.148	0.528	0.445	0.487
k_{sm14}	0.016	0.021	0.019	0.015	0.020	0.018	0.067	0.075	0.071
k_{sm12}	0.015	0.018	0.017	0.015	0.015	0.015	0.065	0.071	0.068
k_{sm10}	0.010	0.011	0.012	0.010	0.010	0.010	0.053	0.041	0.047
k_{b6}	0.006	0.008	0.007	0.006	0.009	0.008	0.029	0.025	0.027
k_{b7}	0.008	0.009	0.009	0.007	0.008	0.008	0.019	0.032	0.026
k_{u6}	-0.006	-0.005	-0.006	-0.005	-0.006	-0.006	-0.024	-0.016	-0.020
k_{u7}	-0.002	-0.009	-0.006	-0.001	-0.009	-0.005	-0.008	-0.031	-0.020
k_{b9}	0.007	0.000	0.004	0.006	0.002	0.004	0.022	0.013	0.018
k_{u8}	-0.007	-0.000	-0.004	-0.006	-0.001	-0.004	-0.020	-0.009	-0.015
k_{b8}	0.010	0.007	0.009	0.009	0.006	0.008	0.014	0.012	0.013
k_{u9}	0.001	0.001	0.001	0.000	-0.000	0.000	-0.013	-0.005	-0.009

https://doi.org/10.1371/journal.pone.0228967.t005

Both the parameters k_{b8} and k_{u8} are related to the activation of the secondary binding site S1. Here, k_{b8} and k_{u8} together with k_{sm12} effectively controls transcription from active state of S1. Due to the close proximity of S1 and S2, transcription rate from S2 shows similar sensitivity as from S1, i.e., $k_{sm12} \sim k_{sm14}$. The transcription rate k_{sm10} from the distal binding site P2 shows a low correlation with the output compared to transcription from other binding sites. The parameter set k_{b6} and k_{u6} related to the activation of the primary binding site P1 shows low correlation. However, when activated the same site ($P1^*$) starts producing the transcripts with maximum efficiency. Thus, activation of P1 serves as a bottleneck for *narK2* transcripts.

Table 6. CC, RCC, PRCC values for all the parameter of *Rv1738*. The input parameters are calculated with output GFP using 5% perturbation.

	CC			RCC			PRCC		
Parameter	Set1	Set2	Mean	Set1	Set2	Mean	Set1	Set2	Mean
k_{dm}	-0.548	-0.550	-0.549	-0.529	-0.531	-0.530	-0.899	-0.898	-0.899
k_{sm19}	0.219	0.221	0.220	0.208	0.213	0.211	0.632	0.625	0.629
k_{sm17}	0.153	0.177	0.165	0.148	0.171	0.160	0.494	0.552	0.523
k_{sm11}	0.139	0.113	0.126	0.135	0.108	0.122	0.453	0.384	0.419
k_{sm15}	0.016	0.017	0.017	0.015	0.017	0.016	0.070	0.065	0.068
k_{sm9}	0.020	0.021	0.021	0.020	0.020	0.020	0.060	0.062	0.061
k_{b7}	0.006	0.016	0.011	0.004	0.015	0.010	0.035	0.039	0.037
k_{u7}	-0.010	-0.005	-0.008	-0.009	-0.004	-0.006	-0.026	-0.033	-0.030
k_{u8}	-0.005	-0.003	-0.004	-0.006	-0.003	-0.005	-0.019	-0.015	-0.017
k_{b6}	0.003	0.004	0.004	0.003	0.004	0.004	0.016	0.011	0.014
k_{u6}	-0.000	-0.007	-0.004	-0.001	-0.006	-0.004	-0.016	-0.011	-0.014
k_{b9}	0.004	0.001	0.003	0.003	0.001	0.002	0.018	0.009	0.014
k_{b8}	0.003	0.003	0.003	0.003	0.002	0.003	0.017	0.008	0.013
k_{u9}	-0.005	-0.003	-0.004	-0.006	-0.002	-0.004	-0.017	-0.005	-0.011
k_{sm13}	0.005	0.001	0.003	0.005	0.000	0.003	0.007	0.009	0.008

https://doi.org/10.1371/journal.pone.0228967.t006

On a similar note, the parameter sets (k_{b7}, k_{u7}) and (k_{b9}, k_{u9}) controls the activation of the sites P2 and S2, respectively.

In *Rv1738*, the ordering of the parameters in terms of correlation values (absolute) are (see Table 6)

$$k_{sm19} > k_{sm17} > k_{sm11} \gg k_{sm15} \sim k_{sm9} > k_{b7} \sim k_{u7} > k_{u8} \sim k_{b6} \sim k_{u6} \sim k_{b9} \sim k_{b8} \sim k_{u9} \sim k_{sm13}.$$

The above ordering of correlation values associated with *Rv1738* suggests that the most sensitive parameter is k_{sm19}, the transcription rate controlled by both P2 and S2, proximal to *Rv1738*. The parameter k_{sm17} reflects the co-operative effect of P1 and S1, however, distal binding sites for the same gene. Thus mutation at P2 drastically lowers down the GFP expression as observed in pBmutP2. Experimentally such signature is observed in the mutant pBmutP1P2 [7] (see Fig 3D). It is important to note that the said mutant also affects the GFP expression profile of *narK2*, where it has been labelled as pAmutP1P2. Both the mutants pAmutP1P2 and pBmutP1P2 are same as, as in both cases P1 and P2 site is mutated [7]. For the sake of labelling, they have been named differently. The next sensitive parameter is k_{sm11} and is due to the binding site P2 alone. Role of the binding site S2 gets reflected through k_{sm15}, which appears next in the ordering. The sensitivity of transcription rate k_{sm9} from distal binding site P1 (for *Rv1738*) reduces further and has a weak role in the overall production of transcripts. The weak contribution of P1 is observed in the expression profile of the mutant pBmutP1 [7]. We again note here that the mutant pBmutP1 is same as pAmutP1 (labelled for *narK2*). Transcription rate k_{sm13} from distal secondary site S2 is least and appears at the end of ordering. In between k_{sm9} and k_{sm13}, the sensitivity of different binding rates appear.

High correlation results into high sensitivity amplification

The results reported in the previous subsection suggest that for each target gene, few rate parameters show a high correlation with the GFP level compared to the rest of the parameters. It is thus interesting to inspect whether the same parameter plays a crucial role in sensitivity amplification. To this end we calculate sensitivity amplification for all the parameters related to *Rv3134c*, *hspX* and *narK2-Rv1738*. The parameters with a high correlation coefficient with the output (GFP) indeed show a high level of sensitivity amplification (see Fig 5). On the other hand, the other parameters play little role in doing so (see S5–S8 Figs).

The parameter k_{sm3} represents co-operativity driven mRNA production rate in *Rv3134c* with highest value of PRCC (see Table 3). It shows highest level of sensitivity amplification compared to other parameters related to *Rv3134c*. In *hspX*, k_{sm4} and k_{sm7} show maximum correlation with output. k_{sm4} is related to gene expression regulated by P1 whereas co-operative effect of P1, S and P2 gets reflected through k_{sm7}. Both these parameters show high level of sensitivity amplification of the output.

In *narK2*, the transcription rate k_{sm8} shows the maximum correlation with output and plays a decisive role in gene expression. The similar feature is observed in the calculation of sensitivity amplification. Interestingly, for *Rv1738* the proximal binding sites, P2 and S2 mainly control its expression and is reflected through a high level of transcription rate k_{sm19}. A high correlation value of k_{sm19} with the output also gets reflected in sensitivity amplification.

Conclusion

In the present work, we focused on the sensitivity of the kinetic parameters relevant to the DevR regulated gene expression in *M. tuberculosis*. To this end, a mathematical model is presented based on kinetic interactions between DevR and four target genes. We carried out

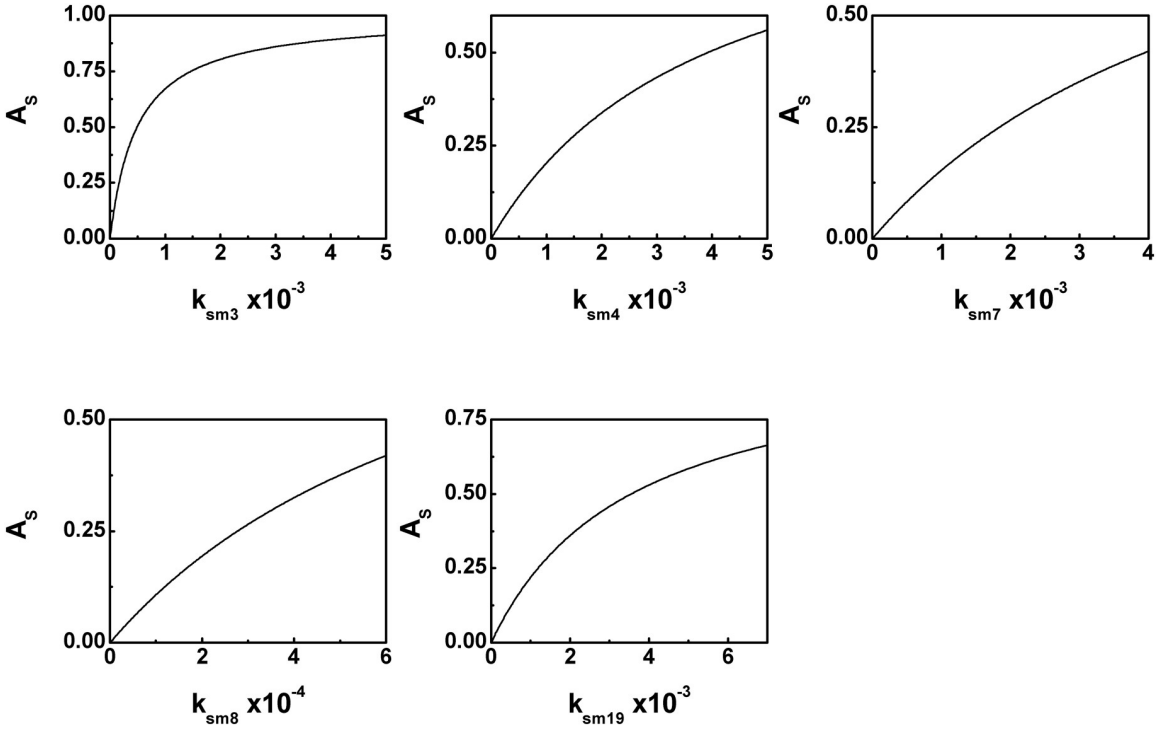

Fig 5. Sensitivity amplification of transcription rate. Sensitivity amplification as a function of parameters with high value of correlation coefficients. k_{sm3} is the transcription rate of *Rv3134c*. k_{sm4} and k_{sm7} are the transcription rates associated with *hspX*. k_{sm8} and k_{sm19} control the transcription of *narK2* and *Rv1738*, respectively.

https://doi.org/10.1371/journal.pone.0228967.g005

stochastic optimization to obtain the physiologically relevant parameter set that can reproduce the experimental profiles. A systematic study based on sensitivity analysis is performed, which reveals the ordering of the parameters based on their correlation values with the output, i.e., GFP concentration. Together with the experimental information, our analysis provides information about the prime steps of DevR controlled gene regulation under dormancy. Sensitivity analysis reveals that the transcription rates are the crucial step in the kinetics and is further supported by sensitivity amplification. The ordering of parameters provides a guideline to tackle virulence by a proper mutation that controls the process of transcription during dormancy related gene expression in *M. tuberculosis*. The present study may work as a reference for the experimentalist to carry out further research on DevR regulated networks that are yet to be explored.

Supporting information

S1 Text. Supplementary information. Kinetic scheme and equations for phosphorylated DevR regulated gene expression. The text contains detailed scheme and differential equations for the model.
(PDF)

S1 Fig. Optimization profiles of kinetic parameters associated with *Rv3134c*. The perturbed parameter is ploted as a function of SA steps. In each panel, the five colored lines originated from different SA simulation. The horizontal dotted lines is for the base parameter value reported in Table 1.
(PDF)

S2 Fig. Optimization profiles of kinetic parameters associated with *hspX*. The perturbed parameter is ploted as a function of SA steps. In each panel, the five colored lines originated from different SA simulation. The horizontal dotted lines is for the base parameter value reported in Table 1.
(PDF)

S3 Fig. Optimization profiles of kinetic parameters associated with *narK2-Rv1738*. The perturbed parameter is ploted as a function of SA steps. In each panel, the five colored lines originated from different SA simulation. The horizontal dotted lines is for the base parameter value reported in Table 1.
(PDF)

S4 Fig. Scatter plots. The output (GFP in nM) as a function of synthesis and degradation rates of phosphorylated DevR (k_{srp} and k_{drp}) and GFP (k_{sg} and k_{dg}). Each panel consists of 10^3 independent simulation data.
(PDF)

S5 Fig. Sensitivity amplification of parameters related to *Rv3134c*.
(PDF)

S6 Fig. Sensitivity amplification of parameters related to *hspX*.
(PDF)

S7 Fig. Sensitivity amplification of parameters related to *narK2*.
(PDF)

S8 Fig. Sensitivity amplification of parameters related to *Rv1738*.
(PDF)

S1 Table. Kinetic parameters. List of all kinetic parameters used in the model.
(PDF)

S2 Table. CC, RCC, PRCC values. Various correlation coefficient values are obtained by using 10% perturbation and 10^5 indipendent run for synthesis and degradation rate parameters of four genes.
(PDF)

S3 Table. CC, RCC, PRCC values. Various correlation coefficient values are obtained by using 10% perturbation and 10^5 indipendent run for all the input parameter with output of *Rv3134c*.
(PDF)

S4 Table. CC, RCC, PRCC values. Various correlation coefficient values are obtained by using 10% perturbation and 10^5 indipendent run for all the input parameter with output of *hspX*.
(PDF)

S5 Table. CC, RCC, PRCC values. Various correlation coefficient values are obtained by using 10% perturbation and 10^5 indipendent run for all the input parameter with output of *narK2*.
(PDF)

S6 Table. CC, RCC, PRCC values. Various correlation coefficient values are obtained by using 10% perturbation and 10^5 indipendent run for all the input parameter with output of *Rv1738*.
(PDF)

Author Contributions

Conceptualization: Jagannath Das, Suman K. Banik.

Formal analysis: Jagannath Das, Tarunendu Mapder, Sudip Chattopadhyay, Suman K. Banik.

Resources: Sudip Chattopadhyay, Suman K. Banik.

Supervision: Sudip Chattopadhyay, Suman K. Banik.

Writing – original draft: Jagannath Das, Tarunendu Mapder, Sudip Chattopadhyay, Suman K. Banik.

References

1. World Health Organisation. Tuberculosis (www.who.int/news-room/fact-sheets/detail/tuberculosis),; 2019.
2. Appleby JL, Parkinson JS, Bourret RB. Signal transduction via the multi-step phosphorelay: not necessarily a road less traveled. Cell. 1996; 86:845–848. https://doi.org/10.1016/s0092-8674(00)80158-0 PMID: 8808618
3. Hoch JA. Two-component and phosphorelay signal transduction. Curr Opin Microbiol. 2000; 3:165–170. https://doi.org/10.1016/s1369-5274(00)00070-9 PMID: 10745001
4. Stock AM, Robinson VL, Goudreau PN. Two-component signal transduction. Annu Rev Biochem. 2000; 69:183–215. https://doi.org/10.1146/annurev.biochem.69.1.183 PMID: 10966457
5. Bretl DJ, Demetriadou C, Zahrt TC. Adaptation to environmental stimuli within the host: two-component signal transduction systems of Mycobacterium tuberculosis. Microbiol Mol Biol Rev. 2011; 75:566–582. https://doi.org/10.1128/MMBR.05004-11 PMID: 22126994
6. Chauhan S, Sharma D, Singh A, Surolia A, Tyagi JS. Comprehensive insights into Mycobacterium tuberculosis DevR (DosR) regulon activation switch. Nucleic Acids Res. 2011; 39:7400–7414. https://doi.org/10.1093/nar/gkr375 PMID: 21653552
7. Chauhan S, Tyagi JS. Interaction of DevR with multiple binding sites synergistically activates divergent transcription of narK2-Rv1738 genes in Mycobacterium tuberculosis. J Bacteriol. 2008; 190:5394–5403. https://doi.org/10.1128/JB.00488-08 PMID: 18502855
8. Kohar V, Lu M. Role of noise and parametric variation in the dynamics of gene regulatory circuits. NPJ Syst Biol Appl. 2018; 4:40. https://doi.org/10.1038/s41540-018-0076-x PMID: 30416751
9. Feng XJ, Hooshangi S, Chen D, Li G, Weiss R, Rabitz H. Optimizing genetic circuits by global sensitivity analysis. Biophys J. 2004; 87:2195–2202. https://doi.org/10.1529/biophysj.104.044131 PMID: 15454422
10. Meir E, von Dassow G, Munro E, Odell GM. Robustness, flexibility, and the role of lateral inhibition in the neurogenic network. Curr Biol. 2002; 12:778–786. https://doi.org/10.1016/s0960-9822(02)00839-4 PMID: 12015114
11. Leon M, Woods ML, Fedorec AJ, Barnes CP. A computational method for the investigation of multistable systems and its application to genetic switches. BMC Syst Biol. 2016; 10:130. https://doi.org/10.1186/s12918-016-0375-z PMID: 27927198
12. Bandyopadhyay A, Biswas S, Maity AK, Banik SK. Analysis of DevR regulated genes in Mycobacterium tuberculosis. Syst Synth Biol. 2014; 8:3–20. https://doi.org/10.1007/s11693-014-9133-y PMID: 24592287
13. Kirkpatrick S, Gelatt CD, Vecchi MP. Optimization by Simulated Annealing. Science. 1983; 220:671–680. https://doi.org/10.1126/science.220.4598.671 PMID: 17813860
14. Kirkpatrick S. Optimization by simulated annealing: Quantitative studies. J Stat Phys. 1984; 34:975–986. https://doi.org/10.1007/BF01009452
15. Metropolis N, Rosenbluth AW, Rosenbluth MN, Teller AH, Teller E. Equation of State Calculations by Fast Computing Machines. J Chem Phys. 1953; 21:1087–1092. https://doi.org/10.1063/1.1699114
16. Salteli A, Tarantola S, Campolongo F, Ratto M. Sensitivity Analysis in Practice: A Guide to Assessing Scientific Models. John Wiley, New Jersy; 2004.
17. Saltelli A, Ratto M, Tarantola S, Campolongo F. Sensitivity analysis for chemical models. Chem Rev. 2005; 105:2811–2828. https://doi.org/10.1021/cr040659d PMID: 16011325
18. Marino S, Hogue IB, Ray CJ, Kirschner DE. A methodology for performing global uncertainty and sensitivity analysis in systems biology. J Theor Biol. 2008; 254:178–196. https://doi.org/10.1016/j.jtbi.2008.04.011 PMID: 18572196

19. Talukder S, Sen S, Metzler R, Banik SK, Chaudhury P. Stochastic optimization-based study of dimerization kinetics. J Chem Sci. 2013; 125:1619–1627. https://doi.org/10.1007/s12039-013-0502-y

20. Mapder T, Talukder S, Chattopadhyay S, Banik SK. Deciphering Parameter Sensitivity in the BvgAS Signal Transduction. PLoS ONE. 2016; 11:e0147281. https://doi.org/10.1371/journal.pone.0147281 PMID: 26812153

21. Savageau MA. Biochemical Systems Analysis: A Study of Function and Design in Molecular Biology. Addison-Wesley, Reading, Massachusetts; 1976.

22. Koshland DE, Goldbeter A, Stock JB. Amplification and adaptation in regulatory and sensory systems. Science. 1982; 217:220–225.

23. Goldbeter A, Koshland DE. Sensitivity amplification in biochemical systems. Q Rev Biophys. 1982; 15:555–591. https://doi.org/10.1017/s0033583500003449 PMID: 6294720

24. Park HD, Guinn KM, Harrell MI, Liao R, Voskuil MI, Tompa M, et al. Rv3133c/dosR is a transcription factor that mediates the hypoxic response of Mycobacterium tuberculosis. Mol Microbiol. 2003; 48:833–843. https://doi.org/10.1046/j.1365-2958.2003.03474.x PMID: 12694625

25. Monod J. The growth of bacterial cultures. Ann Rev Microbiol. 1949; 3:371–394. https://doi.org/10.1146/annurev.mi.03.100149.002103

26. Chauhan S, Tyagi JS. Cooperative binding of phosphorylated DevR to upstream sites is necessary and sufficient for activation of the Rv3134c-devRS operon in Mycobacterium tuberculosis: implication in the induction of DevR target genes. J Bacteriol. 2008; 190:4301–4312. https://doi.org/10.1128/JB.01308-07 PMID: 18359816